Monthly Notices of the ROYAL ASTRONOMICAL SOCIETY

Mon. Not. R. Astron. Soc. **409,** 1002–1012 (2010) doi:10.1111/j.1365-2966.2010.17355.x

IC 2602: a lithium depletion boundary age and new candidate low-mass stellar members★

P. D. Dobbie,[1,2]† N. Lodieu[3,4] and R. G. Sharp[1,2]

[1]*Anglo-Australian Observatory, PO Box 296, Epping, NSW, 1710, Australia*
[2]*Australian Astronomical Observatory, PO Box 296, Epping, NSW, 1710, Australia*
[3]*Instituto de Astrofísica de Canarias, Vía Láctea s/n, E-38200 La Laguna, Tenerife, Spain*
[4]*Departmento de Astrofísica, Universidad de La Laguna, E-38205 La Laguna, Tenerife, Spain*

Accepted 2010 July 13. Received 2010 July 13; in original form 2010 March 22

ABSTRACT

We report the results from a photometric and spectroscopic survey of ∼1.4 deg^2 of the young open cluster IC 2602. Fourteen objects have been identified as having magnitudes, spectral types and radial velocities consistent with being probable or possible low-mass stellar members of the cluster. We have used the observed location of the lithium depletion boundary in the sequence defined by these objects to place a new and improved constraint on the cluster age, $\tau = 46^{+6}_{-5}$ Myr. This new determination is larger by a factor ∼1.3–1.8 than the majority of age estimates which have been obtained using the main-sequence turn-off or pre-main-sequence isochrone techniques. It is thus consistent with the trend indicated by the results of similar studies on other young open clusters. Based on this new age, we set a lower limit on the cluster mass function over the range $M = 0.054 - 0.24\,\mathrm{M}_{\odot}$, $\mathrm{d}n/\mathrm{d}M > 46\,\mathrm{M}_{\odot}^{-1}$. If the mass function of IC 2602 has a form similar to that of other young clusters and associations then future wide, deep surveys can expect to unearth at least a handful of brown dwarfs which could potentially serve as benchmark objects.

Key words: techniques: photometric – brown dwarfs – stars: low-mass – open clusters and associations: individual: IC 2602.

1 INTRODUCTION

Open clusters represent coeval families of stars residing at similar heliocentric distances, that formed from molecular gas clouds with near uniform chemical composition. The common properties of the members of these populations render them excellent targets for addressing fundamental questions in stellar astrophysics. For example, they are frequently utilized to investigate the forms of the stellar/substellar initial mass function (e.g. Dobbie et al. 2002; Kroupa 2002; Chabrier 2003; Moraux, Bouvier & Clarke 2005; Lodieu et al. 2007a, 2009) and the stellar initial mass–final mass relation (e.g. Weidemann 2000; Williams, Bolte & Koester 2004; Kalirai et al. 2005; Dobbie et al. 2006, 2009). Open cluster members are also widely used to probe stellar magnetism (e.g. Barnes et al. 2001; Marsden et al. 2005), the evolution of stellar angular momentum (e.g. Irwin et al. 2008, 2009) and the mixing processes which occur within stars (e.g. Pinsonneault 1997; Jeffries & James 1999; King et al. 2010).

The success of many of these types of investigation is influenced by the level of accuracy with which the ages of the populations under scrutiny are known. Robust age determinations permit meaningful comparisons to be drawn between the measured properties of the members of different clusters (e.g. the abundance of lithium in stars of different effective temperature as a function of age; Randich et al. 2001) and aid in the judicious interpretation of the observed trends in a theoretical context. Most existing open cluster age estimates have been obtained using the main-sequence turn-off technique (MSTO), where the observed location in the luminosity–temperature plane of stars at the end of their main-sequence life is compared to the predictions of stellar evolutionary models (Meynet, Mermilliod & Maeder 1993). However, for all but the oldest populations these age estimates are muddied by uncertainties associated with the extra convective mixing which is believed to occur at the boundary between the cores of stars and the overlying layers (Woo & Demarque 2001). The degree of convective core overshooting adopted in stellar evolutionary models impacts both the predicted main-sequence lifetimes and the luminosities of stars, with greater overshoot leading to larger cluster age estimates. While several lines of observational evidence are consistent with moderate levels of convective overshooting across a broad range of main-sequence masses (Claret 1997), a method of determining open cluster ages

★Based on observations made with Anglo-Australian Telescope at Siding Spring Observatory, Australia.
†E-mail: pdd@aao.gov.au

which is independent of assumptions about the physics of the core boundary is to be preferred.

Fortunately, such a technique has been successfully demonstrated by Basri, Marcy & Graham (1996). It relies on locating the boundary, in terms of mass, at which lithium reappears in the spectral energy distributions of the completely convective very low mass stellar and substellar members of a population (Rebolo, Martín & Magazzù 1992). As a population matures, up to $\tau \sim 300$ Myr, the location of this lithium depletion boundary migrates to lower mass (corresponding to later spectral types), providing a potentially excellent handle on the age (D'Antona & Mazzitelli 1994). However, since this approach is reliant on the availability of moderate signal-to-noise ratio medium resolution optical spectroscopy of intrinsically faint red objects, as of today, there are only five young open clusters with lithium depletion boundary based age determinations. These are, in order of increasing youth, the Pleiades (125 ± 8 Myr; Stauffer, Schultz & Kirkpatrick 1998a; Barrado y Navascués, Stauffer & Jayawardhana 2004), Alpha Persei (85 ± 10 Myr; Barrado y Navascués et al. 2002, 2004), IC 2391 (50 ± 5 Myr; Barrado y Navascués, Stauffer & Patten 1999, Barrado y Navascués et al. 2004), NGC 2547 (35 ± 4 Myr; Jeffries et al. 2003; Oliveira et al. 2003; Jeffries & Oliveira 2005) and IC 4665 (28 ± 5 Myr; Manzi et al. 2008). It is worth noting that while the ages estimated from this method tend to be slightly larger than the ages derived from the MSTO technique (Mermilliod 1981; Naylor et al. 2002; Jeffries & Oliveira 2005) this is not always the case e.g. IC 4665 (Manzi et al. 2008).

IC 2602 is an important pre-main-sequence southern open cluster which is located at a similar distance ($d = 150$–170 pc; e.g. Braes 1961; Nicolet 1981; Robichon et al. 1999; Kharchenko et al. 2005) and is of comparable age (30–67 Myr; Kharchenko et al. 2005) to IC 2391. The most recent distance estimate based on a revised reduction of the *Hipparcos* data indicates $d = 148.6 \pm 2.1$ pc (van Leeuwen 2009). This is the value we adopt here for our subsequent analysis. The cluster has a metallicity close to the solar value ([Fe/H] $= -0.05 \pm 0.05$; Randich et al. 2001) and foreground reddening is low, e.g. $E(B - V) = 0.035 \pm 0.01$ (Hill & Perry 1969), $E(B - V) = 0.021 \pm 0.013$ (Nicolet 1981). The cluster is located close to the Galactic plane ($b = -4.^{\circ}9$) and this has led to significant difficulties in distinguishing members from reddened background field stars via photometric surveys. Current known low-mass members are limited to late-K and early-M dwarfs identified using combinations of X-ray (Randich et al. 1995) and optical (*BVI*) photometry (Prosser, Randich & Stauffer 1996) and optical spectroscopy (e.g. Randich et al. 1997; Stauffer et al. 1997; Barnes et al. 1999). Moreover, the cluster exhibits only a small proper motion, hence only a few bright members have been confirmed astrometrically (Braes 1961). Despite the youth and proximity of IC 2602, no brown dwarf members have been reported to date.

In this paper, we present a new lithium depletion boundary age estimate for IC 2602 which is based on data obtained with the AAOmega multifibre optical spectrograph mounted on the Anglo-Australian Telescope. In Section 2, we define the sample of sources observed at medium resolution with AAOmega and describe the spectroscopic follow-up observations. In Section 3, we present a spectral analysis to assign membership based on spectral shape, the strength of Hα emission and radial velocities, and to search for the presence of lithium. The membership status of key objects is further scrutinized via proper motion measurements. Finally, we discuss the discovery of new low-mass stellar members and put into context our new age estimate of IC 2602 in Section 4.

Table 1. Summary of the 2.2 m + WFI optical imaging data obtained from the ESO archive.

Field ID	RA (J2000.0)	Dec. (J2000.0)	Exp. time (s)
IC 2602_11	10 38 49.7	−64 23 13	60, 600
IC 2602_15	10 38 49.8	−64 53 12	60, 600
IC 2602_BX	10 41 34.4	−64 08 50	60, 600
IC 2602_B4	10 41 35.1	−64 30 36	60, 600
IC 2602_14	10 43 19.8	−64 53 12	60, 600
IC 2602_B2	10 45 34.2	−64 15 35	60, 600

2 OBSERVATIONS AND SELECTION OF TARGETS

2.1 Optical and near-IR photometry

We have retrieved *I*-band imaging for ∼1.4 deg^2 of IC 2602 from the European Southern Observatory (ESO) data archive.[1] These observations were undertaken on the nights of 2001 February 12–13 with the Wide Field Imager (WFI; Baade et al. 1999) and the 2.2-m telescope which is located at La Silla, Chile. The ESO WFI consists of a mosaic of eight EEV 4096 × 2048 pixel charge coupled devices (CCDs) which covers an area of 34 × 33 arcmin^2 in each pointing. Data from six overlapping pointings (Table 1) were reduced using the Cambridge Astronomical Survey Unit CCD reduction toolkit (Irwin & Lewis 2001) to follow standard procedures, namely, subtraction of the bias, flat-fielding and astrometric calibration. Subsequently, aperture photometry was performed on the reduced images using a circular window with a diameter of 1.5 × the full width half maximum of the mean point spread function (∼1–1.5 arcsec) and sources morphologically classified.

The instrumental magnitudes of stars in the shallow and the deep images and in the overlapping regions of the different pointings were examined and found to exhibit only small differences from data set to data set ($\lesssim$2 per cent). This was taken to indicate that the sky was largely clear when these observations were acquired. We applied small offsets to the photometry from the shallow images and that from the deep five fields surrounding the central pointing (IC 2602_B4) to ensure the instrumental magnitudes achieved a high level of internal consistency. Subsequently, to convert the instrumental magnitudes on to the Ic/Iwp_ESO845 natural system, we adopted zero-point and airmass coefficients of $k_0 = 23.06$[2] and $k_1 = 0.02$,[3] respectively. Although a rigorous photometric calibration of these data has not been performed, we believe these magnitudes to be accurate to <10 per cent, which is sufficient for our purposes.

Near-IR photometry for IC 2602 was obtained by querying the Two Micron All Sky Survey (2MASS) All Sky Point Source Catalogue (Cutri et al. 2003; Skrutskie et al. 2006). The 2MASS detections were cross-matched with sources in the WFI images using the STARLINK routine TOPCAT and a matching radius of 1.5 arcsec. Subsequently, these data were used to construct an $I - J$, J colour–magnitude diagram (CMD) for the cluster (Fig. 1).

[1] http://archive.eso.org/cms/
[2] www.eso.org/sci/facilities/lasilla/instruments/wfi/inst/zeropoints/ColorEquations/
[3] www.eso.org/sci/facilities/lasilla/telescopes/d1p5/misc/Extinction.html

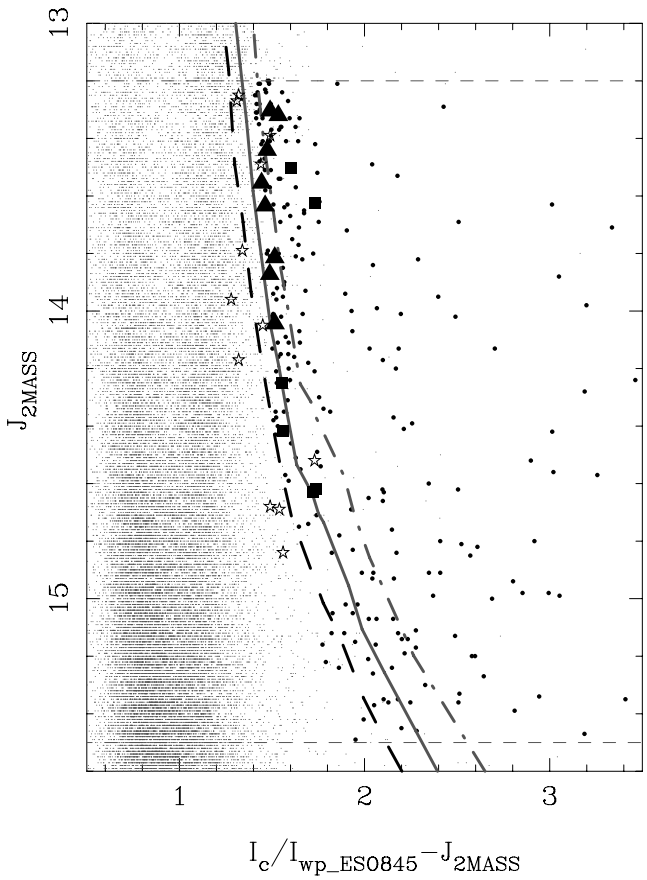

Figure 1. An $I-J, J$ colour-magnitude diagram for all objects classified as stellar in the ESO WFI field of view and which have a 2MASS counterpart. As a guide to the location of the cluster sequence, we have overplotted a selection of Pleiades low-mass stars (open stars) and a NextGen theoretical isochrone for 50 Myr (dashed line), both shifted to the distance of IC 2602. Objects which were selected for optical spectroscopy are highlighted (large dots) as are spectroscopic members with (filled squares) and without (filled triangles) lithium in absorption at 6707.8 Å. 20- and 32-Myr theoretical NextGen isochrones, adjusted as per the 50 Myr model, are also shown (solid and dot–dashed grey lines, respectively). The latter provides a good match to the position of the candidate members around the lithium depletion boundary.

2.2 Selection of candidate low-mass members of IC 2602

An $I-J, J$ CMD for all objects classified as stellar in the optical data and with a counterpart in the 2MASS catalogue is shown in Fig. 1. As a guide to the likely location of the IC 2602 sequence, we overplotted a selection of low-mass stellar members of the Pleiades for which V, I and J photometry are available in the literature (Stauffer, Hamilton & Probst 1994; Stauffer et al. 1998b). The I-band photometry of the Pleiades sequence has been transformed on to the Ic/Iwp_ESO845 system using colour equations given in the WFI User Manual.[4] This sequence was then shifted (from an assumed $d = 135$ pc; Pan, Shao & Kulkarni 2004) to the new *Hipparcos* distance of IC 2602 and adjusted by 0.45 mag to larger luminosities [based on the predictions of the Baraffe et al. (1998) models] to account for the expected lower age of this cluster (i.e. similar to the age of IC 2391). Extinction was neglected here since IC 2602 and the Pleiades have similar very low levels of foreground reddening. A theoretical isochrone for 50 Myr (Baraffe et al. 1998) has also be been overplotted to provide further guidance to the probable location of the cluster sequence. The NextGen I-band magnitudes were transformed on to the Ic/Iwp_ESO845 system following the same method as was used for the Pleiades objects and the model J-band photometry transformed to the 2MASS system using the colour equations listed in Carpenter (2001). This isochrone was then shifted to account for the distance to and foreground reddening towards IC 2602, i.e. $E(B-V) = 0.035$, (Hill & Perry 1969) and $A_I/E(B-V) = 1.57$, $A_J/E(B-V) = 0.86$ (Fitzpatrick 1999).

Noting the minimum (∼30 Myr) and the maximum (∼67 Myr) nuclear-based age estimates for IC 2602 in the recent literature and using theoretical data from Chabrier & Baraffe (1997) and Baraffe et al. (1998), we estimated the likely magnitude range within which the lithium depletion boundary should lie to be $J \sim 13.2$–15.5 mag. These limits are shown by the top and bottom horizontal dashed lines in Fig. 1, respectively. Given the particularly high density of field stars in this direction and the lack of an obvious cluster sequence, we selected all stellar objects between $J \sim 13.2$–15.5 mag that lie redwards of a line loosely defined by the middle of the sequence of Pleiades objects (open stars in Fig. 1) and the 50-Myr theoretical isochrone. Selection of objects located even slightly further to the blue would have resulted in much too large a sample of objects to follow-up spectroscopically within our allocated time. The line of our cut is approximately one magnitude more luminous than the field sequence at the distance of IC 2602, so for an unreddened main-sequence dwarf to fall into our sample it would have to be at $d \lesssim 100$ pc. Our initial selection criteria lead to the identification of 348 candidate low-mass members of IC 2602. However, as a final step prior to configuring AAOmega, the I- and J-band images of all candidates were visually inspected. Many of the reddest objects in the CMD were found to be unresolved blends in the 2MASS imaging. These and other objects where the photometry was probably affected by image artefacts, were eliminated. This left a list of 249 candidate low-mass members of IC 2602 for spectroscopic follow-up (small solid circles in Fig. 1).

2.3 AAOmega spectroscopic observations

We used the AAOmega (Sharp et al. 2006) and the 2dF facility (Lewis et al. 2002) to obtain medium-resolution (R∼3500) optical spectroscopy for the bulk of our candidate low-mass members of IC 2602. The 2° field of view and ∼400 fibre multiplex of the 2dF–AAOmega system makes it the most efficient system available for our purposes. The ∼2 arcsec fibres, which can be placed with a minimum separation of ∼30 arcsec on the sky (Miszalski et al. 2006), feed the dual-beam AAOmega spectrograph (Saunders et al. 2004). A single-fibre configuration was observed on the night of 2010 February 23 between 13 h and 15h15 UT in cloudless conditions, with seeing in the range 1.0–1.5 arcsec and with the moon at ∼65 per cent illumination.

The 1000R grating was employed in the red arm, which delivered $R \sim 3500$ over the 6200–7320 Å wavelength range (the exact wavelength coverage depends slightly on the position of the fibre on the spectrograph slit). Four individual integrations of 1800 s were obtained, for a total on-source exposure time of 2 h. These science observations were bracketed by flat-field and arc (a blend of CuAr+FeAr, He and Ne) calibration frames. Simultaneous observations from the blue arm are not considered in this work. 30 science fibres were allocated to previously determined blank sky positions, distributed across the field of view, to provide a simultaneous estimation of the sky spectrum for background subtraction.

[4] www.eso.org/sci/facilities/lasilla/instruments/wfi/doc/index.html

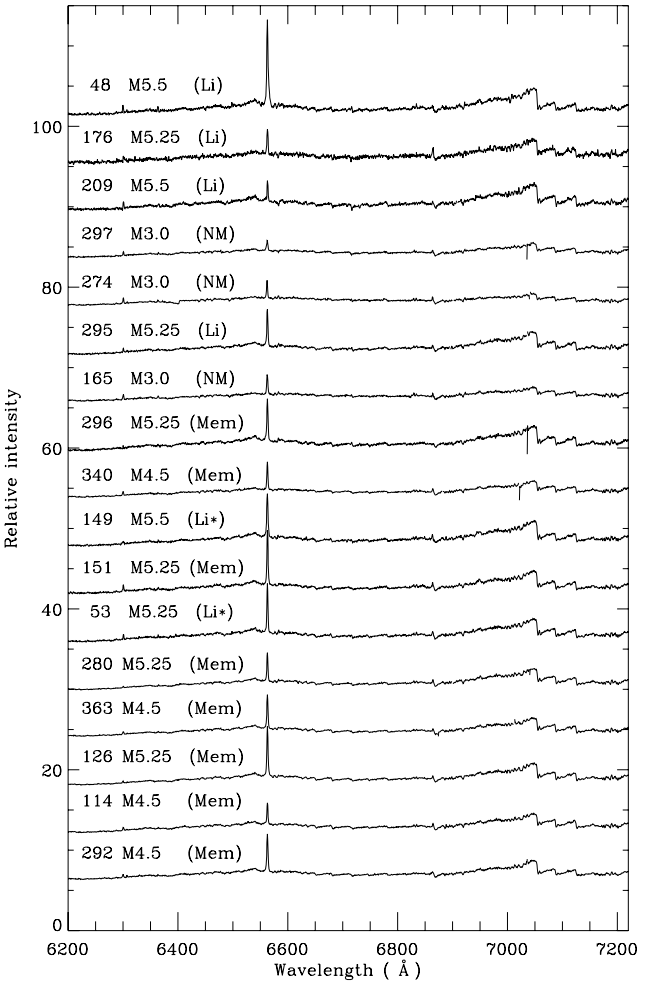

Figure 2. AAOmega optical spectra of the 17 objects initially identified as candidate members of IC 2602, prior to our radial velocity analysis. The wavelength coverage spans 6200–7220 Å and the mean resolution is $R \sim 3500$. Spectra are plotted by increasing *I*-band magnitudes (decreasing brightness) but are offset for clarity. Possible binary objects are highlighted (*).

The data were reduced in the standard manner using the 2DFDR package provided by the Anglo-Australian Observatory. Inspection of photographic narrow-band images of the cluster obtained with the United Kingdom Schmidt Telescope (UKST; Parker et al. 2005) reveal some relatively weak background Hα emission which, from inspection of this image and of the sky fibre spectra, varies slowly over the AAOmega field of view. Therefore, rather than adopting the basic 2DFDR estimate of the sky background which is calculated by median combining the data from all sky fibres across the field, and alternate approach was adopted. The raw data file header metadata was modified prior to reduction to use only the ~8 sky fibres located closest to each target. An analysis of the residual background subtraction in each of these sky fibres showed a noticeable improvement to the sky subtraction accuracy using this approach.

3 THE LITHIUM DEPLETION BOUNDARY

3.1 Spectral classification

Optical spectroscopy was obtained for the 219 photometric candidate cluster members which were allocated a fibre. A total of 22 objects were found to have energy distributions which resemble mid-M dwarfs. Of this subsample, we have conditionally labelled as candidate members the 17 objects which, on the basis of a by-eye inspection, appear to display strong (equivalent width, EW $\lesssim$ −few Å; Fig. 2) Hα emission (Table 2), as is typical for young, very low mass stars (e.g. Barrado y Navascués et al. 2004). To further examine the membership credentials of these, we have spectroscopically classified them more quantitatively and measured their radial velocities from Hα and by cross-correlating the 6950–7150 Å region of each spectrum against a template data set (2MASS J10430236−6402132). We have rejected as probable non-members the other 202 objects for which an optical spectrum was obtained. The vast majority of these appear be of K or very early M spectral types and are presumably reddened background stars which are known to be an issue for photometric studies of this cluster (e.g. Foster et al. 1997).

We have employed two distinct methods to measure the spectral types of the 17 remaining candidate low-mass members of IC 2602 (Table 3). First, we have computed spectral indices based on the

Table 2. Names of the initial cluster member candidates along with their coordinates, the fibre number assigned to them, the optical *I*-band photometry from the ESO WFI and the 2MASS near-IR magnitudes with their associated error bars.

Designation (2MASS J)	RA (J2000.0)	Dec.	Fibre ID	*I* (WFI)	*J*	*H* (2MASS)	K_S
10422712−6421401	10 42 27.12	−64 21 40.2	292	14.79	13.304 (0.036)	12.707 (0.034)	12.445 (0.034)
10423714−6453308	10 42 37.14	−64 53 30.9	114	14.85	13.320 (0.024)	12.708 (0.030)	12.477 (0.029)
10420463−6434373	10 42 04.64	−64 34 37.3	126	14.92	13.441 (0.025)	12.847 (0.025)	12.627 (0.028)
10464783−6415458	10 46 47.83	−64 15 45.9	363	15.00	13.555 (0.032)	12.930 (0.025)	12.622 (0.032)
10420419−6404236	10 42 04.19	−64 04 23.7	280	15.10	13.634 (0.025)	13.050 (0.028)	12.813 (0.030)
10452984−6444543	10 45 29.84	−64 44 54.3	53	15.11	13.504 (0.024)	12.941 (0.023)	12.582 (0.026)
10405026−6453128	10 40 50.27	−64 53 12.9	151	15.33	13.814 (0.024)	13.217 (0.026)	12.922 (0.026)
10391188−6456046	10 39 11.88	−64 56 04.7	149	15.36	13.624 (0.041)	12.995 (0.040)	12.689 (0.037)
10443357−6415455	10 44 33.57	−64 15 45.6	340	15.36	13.872 (0.026)	13.211 (0.028)	12.928 (0.034)
10430890−6356228	10 43 08.90	−63 56 22.8	296	15.56	14.044 (0.027)	13.454 (0.032)	13.172 (0.037)
10380863−6444337	10 38 08.63	−64 44 33.8	165	15.73	14.208 (0.030)	13.409 (0.027)	13.059 (0.038)
10430236−6402132	10 43 02.36	−64 02 13.2	295	15.80	14.249 (0.045)	13.593 (0.047)	13.299 (0.037)
10413339−6409171	10 41 33.39	−64 09 17.1	274	15.89	14.374 (0.045)	13.724 (0.053)	13.536 (0.060)
10432126−6419594	10 43 21.27	−64 19 59.5	297	15.92	14.354 (0.038)	13.671 (0.036)	13.455 (0.044)
10401542−6426214	10 40 15.43	−64 26 21.5	209	15.98	14.417 (0.040)	13.765 (0.049)	13.482 (0.046)
10370251−6444416	10 37 02.51	−64 44 41.6	176	16.35	14.631 (0.045)	13.895 (0.045)	13.510 (0.048)
10454174−6444037	10 45 41.74	−64 44 03.8	48	16.36	14.619 (0.035)	14.088 (0.022)	13.687 (0.054)

Table 3. TiO5, CaH2 and CaH3 spectral indices measured for our initial 17 candidate members and the corresponding spectral types (SpT). The adopted spectral type is given based on the direct comparison with young spectral templates. The pseudo-EW measurements for the Hα emission line are also listed.

Designation (2MASS J)	TiO5 (SpT)	CaH2 (SpT)	CaH3 (SpT)	SpT	Hα EW (Å)
10422712−6421401	0.34 (4.5)	0.40 (3.7)	0.65 (4.1)	M4.50 (0.25)	−10.4 (0.1)
10423714−6453308	0.37 (4.2)	0.42 (3.5)	0.69 (3.4)	M4.50 (0.25)	−5.0 (0.3)
10420463−6434373	0.32 (4.7)	0.38 (4.1)	0.65 (4.2)	M5.25 (0.25)	−12.4 (0.1)
10464783−6415458	0.34 (4.4)	0.41 (3.6)	0.68 (3.6)	M4.50 (0.25)	−8.8 (0.1)
10420419−6404236	0.33 (4.6)	0.40 (3.7)	0.68 (3.5)	M5.25 (0.25)	−7.1 (0.1)
10452984−6444543	0.29 (5.0)	0.37 (4.1)	0.66 (3.9)	M5.25 (0.25)	−10.8 (0.4)
10405026−6453128	0.29 (4.9)	0.38 (4.0)	0.65 (4.0)	M5.25 (0.25)	−13.2 (0.2)
10391188−6456046	0.28 (5.1)	0.36 (4.4)	0.64 (4.3)	M5.50 (0.25)	−11.4 (0.2)
10443357−6415455	0.44 (3.5)	0.46 (2.9)	0.71 (3.1)	M4.25 (0.25)	−6.2 (0.1)
10430890−6356228	0.28 (5.1)	0.36 (4.3)	0.64 (4.3)	M5.25 (0.25)	−12.5 (0.3)
10380863−6444337	0.52 (2.8)	0.52 (2.2)	0.74 (2.5)	M3.00 (0.50)	−5.0 (0.1)
10430236−6402132	0.30 (4.9)	0.36 (4.3)	0.64 (4.2)	M5.25 (0.25)	−9.4 (0.2)
10413339−6409171	0.52 (2.8)	0.57 (1.6)	0.75 (2.2)	M3.00 (0.50)	−3.9 (0.1)
10432126−6419594	0.46 (3.3)	0.50 (2.4)	0.73 (2.7)	M3.00 (0.50)	−4.1 (0.1)
10401542−6426214	0.28 (5.1)	0.34 (4.7)	0.64 (4.2)	M5.50 (0.25)	−10.1 (0.2)
10370251−6444416	0.37 (4.2)	0.38 (4.0)	0.66 (3.9)	M5.25 (0.25)	−6.6 (0.3)
10454174−6444037	0.24 (5.5)	0.33 (4.8)	0.63 (4.5)	M5.50 (0.25)	−22.8 (0.4)

strengths of the TiO and CaH bands (TiO5, CaH1, CaH2 and CaH3; Reid, Hawley & Gizis 1995; Cruz & Reid 2002) present in the wavelength range covered by our observations. However, these indices are defined from old field dwarfs in the solar neighbourhood (Reid et al. 1995; Cruz & Reid 2002) and may not be perfectly adapted to the spectral classification of young low-mass stars and brown dwarfs. Secondly, we have compared all our spectra to each other in order to define a spectral sequence and then matched them to low-resolution spectroscopy of young M3–M6 dwarfs members of the η Chamaeleontis region (Luhman 2004; Luhman & Steeghs 2004). Interestingly, we have found that the spectral types derived from these stellar and substellar templates are consistently one subclass later than the spectral types inferred from the spectral indices.

We further explored this issue by computing the spectral indices for the young spectral templates. We find that a similar discrepancy exists between the spectral types derived from the spectral indices and the classifications provided in the literature. As members of IC 2602 are likely to be substantially younger than old field dwarfs, we have adopted the spectral types derived from the direct comparison with the η Chamaeleontis objects (τ = 3–10 Myr). These are seen to range from M3.0 to M5.5 (see fifth column of Table 3).

While a substantial proportion of field objects of these spectral types display Hα emission, scrutiny of the large spectroscopic sample studied by West et al. (2008) suggests that only ∼15–20 per cent of M4/M5 dwarfs within 50 pc of the Galactic plane should be expected to have Hα EWs < -6 Å. As our spectroscopic investigation unearthed a total of 16 M4/M5 dwarfs, relative to the field population our sample of candidates members of IC 2602 appears to contain a significant excess (∼10) of these strong Hα emitting objects. Many of these objects appear to lie on a relatively tight sequence, bracketed by the 20 and 50 Myr NextGen theoretical isochrones, in the CMD (Fig. 1).

3.2 Radial velocities

The members of a star cluster have common radial velocities with only a small dispersion ($\delta v_r \lesssim 1\,\mathrm{km\,s^{-1}}$) about the cluster mean value. For IC 2602, the mean radial velocity has been estimated to lie between $\sim$16 km s^{-1} (Randich et al. 2001) and 19 km s^{-1} (Kharchenko et al. 2005). Indeed, very recently Marsden, Carter & Donati (2009) have determined $v_r = 17.4 \pm 1.0\,\mathrm{km\,s^{-1}}$ from their high-resolution study of solar type members. The radial velocities of our 17 candidate low-mass cluster members have been measured, using the SPLOT routine in IRAF to fit a Voigt profile to the observed Hα lines. We note that this analytic profile generally provides a good match to the shape of the observed emission. These measurements have been shifted into the heliocentric rest frame using the routine IRAF RVCORRECT and are shown in Table 4. We have estimated the uncertainties here to be $\sim$7 km s^{-1}, based on the dispersion in radial velocity measurements made from each of the four uncombined spectra of a subsample of the candidates.

Prior to drawing any firm conclusions, we have probed the integrity of our Hα measurements using the IRAF FXCOR routine to determine the radial velocities of the targets with respect to 2MASS J10430236−6402132, the brightest object in our sample to have a location in the J, $I - J$ diagram consistent with the sequence defined by the bulk of the other candidates, an Hα radial velocity within 1σ of the cluster mean, a proper motion consistent with the cluster value (Section 3.4) and a 6707.8-Å lithium absorption line (Section 3.5). We have cross-correlated the 6950–7150 Å region of the spectrum of each object, as favoured by Jeffries & Oliveira (2005), with this template. The resulting velocity estimates have been shifted by $v_r = 17.4\,\mathrm{km\,s^{-1}}$, under the assumption that 2MASS J10430236−6402132 is a bona-fide cluster star, and are shown in Table 4. The errors quoted here are those computed by the FXCOR routine. Based on our measurements of the uncombined spectra, these appear to be a reasonable approximation of the true uncertainties.

Given this level of uncertainty, there appears to be fair agreement between the two different sets of velocities, suggesting that the Hα velocities are reasonable. A cursory glance at these reveals a broad peak in the distribution of objects centred around $\sim$15 km s^{-1}. This likely corresponds to the cluster population. We have chosen to select as radial velocity members those objects which lie within 2σ

Table 4. Radial velocities for our initial 17 candidate members as measured from the central position of the Hα line [$\delta v_r(\mathrm{H}\alpha) = 7\,\mathrm{km\,s^{-1}}$] and by cross-correlation of the 6950–7150 Å spectral region, using 2MASS J10430236−6402132 (fiber 295) as the template*. The mean 0.5–4.5 keV X-ray fluxes (where available in the 2XMMi-DR3 catalogue), the pseudo-EW measurements for the lithium absorption line and relative proper motion measurements based on two CCD epochs, where available, are also shown. Our final decision on the membership of each candidate is given in the last column.

Designation (2MASS J)	v_r(Hα)	v_r(x-corr) (km s^{-1})	0.5–4.5 keV flux mW m^{-2}	Li EW (Å)	$\mu_\alpha \cos\delta$	μ_δ (mas yr^{-1})	Memb?
10422712−6421401	13.7	23.1(5.7)	1.2272 ± 0.1050E-14	≤0.07	−12.1 ± 3.7	7.1 ± 3.4	Y
10423714−6453308	16.4	19.7(4.7)	–	≤0.08			Y
10420463−6434373	14.6	18.4(6.9)	1.6709 ± 0.2360E-14	≤0.07	−11.2 ± 4.8	2.9 ± 6.1	Y
10464783−6415458	14.6	15.9(6.0)	–	≤0.07	–	–	Y
10420419−6404236	12.3	37.4(3.2)	–	≤0.08	–	–	Y?
10452984−6444543	13.7	14.0(4.7)	–	0.41(0.10)	–	–	Y
10405026−6453128	21.0	6.9(6.9)	–	≤0.09	–	–	Y
10391188−6456046	8.2	18.5(6.5)	–	0.45(0.11)	–	–	Y
10443357−6415455	11.4	11.7(5.3)	7.1326 ± 1.5000E-15	≤0.10	–	–	Y?
10430890−6356228	11.9	20.1(5.8)	–	≤0.09	−11.0 ± 4.1	5.9 ± 3.2	Y
10380863−6444337	2.7	5.5(9.5)	–	≤0.09	–	–	N
10430236−6402132	10.9	17.4*	–	0.43(0.11)	−12.1 ± 3.3	7.1 ± 3.3	Y
10413339−6409171	−14.6	−0.1(6.7)	–	≤0.08	–	–	N
10432126−6419594	−1.4	−5.6(5.9)	1.0089 ± 0.4270E-15	≤0.07	−45.1 ± 4.2	−27.5 ± 4.9	N
10401542−6426214	17.3	20.9(6.2)	–	0.56(0.06)	–	–	Y
10370251−6444416	18.7	3.9(13.4)	–	0.29(0.10)	–	–	Y
10454174−6444037	13.7	14.5(5.4)	–	0.61(0.11)	–	–	Y

of the recent Marsden et al. (2009) measurement, i.e. $v_r = 3.4$–$31.4\,\mathrm{km\,s^{-1}}$. While we should expect such a cut to discard only one in ∼20 members, three out of the 17 spectroscopic candidates are rejected outright by us at this stage. These are 2MASS J10432126−6419594, 2MASS J10413339−6409171 and 2MASS J10380863−6444337, the objects which are found to have, by at least 1.5 subclasses, the earliest spectral types (all are M3.0). We note also that while the spectral type and the velocity as measured from the Hα line of 2MASS J10420419−6404236 are consistent with it being a member of IC 2602, the cross-correlation velocity argues against this association. Therefore, for the remainder of this study we consider this object as merely a possible cluster member (see Table 4).

Alone, our broad radial velocity cut does not provide a very stringent membership selection criterion and will admit roughly 30 per cent of field stars (e.g. Kharchenko et al. 2007). Nevertheless, combined, the selection criteria up to this point should reject almost 80–90 per cent of mid-M field stars. If the remaining sample of 14 candidate members was in fact dominated by field dwarfs then, rather than finding a mere 22 stars in the spectroscopic sample with mid-M spectral types, we should have unearthed closer to ∼80 such objects. These would largely represent mid-M dwarfs lying to the foreground of the cluster. We reiterate that as this survey covers only 1.4 deg^2 of the sky and since the cut applied in the CMD corresponds to a field star isochrone at only $d \sim 100$ pc, we have surveyed a relatively small volume of space.

3.3 X-ray fluxes

Young stars are known to be prominent sources of X-ray emission as a result of their active coronae. Randich et al. (1995) present a list of X-ray detections in a 3°.3 × 3°.3 region centred on IC 2602 based on an extended *Roentgen Satellite* (*ROSAT*) Position Sensitive Proportional Counter (PSPC) observation with the *ROSAT* and PSPC. While none of our candidate members appears in their table, it is unlikely that cluster stars at the optical magnitudes in question would have been detected here since the lower X-ray luminosity limit of the *ROSAT* survey is estimated to range from 3×10^{-23} to 3–5×10^{-24} mW at best (∼10^{-2}–10^{-3} count s^{-1} over ∼0.1–2 KeV). However, we note that an X-ray source with a broad-band count rate of $3.146 \pm 0.851 \times 10^{-2}$ count s^{-1} is reported in the second *ROSAT* PSPC catalogue[5] at the position of 2MASS J10422712−6421401, but is flagged as probably spurious and of questionable intensity. If this measurement was to be taken at face value, it would suggest this object was substantially variable and likely flaring at the time of this observation (1993 January 26), consistent with it being identified as a young active late-type star (e.g. Pillitteri et al. 2005).

The central part of our study area has also been imaged at X-ray wavelengths with the *XMM–Newton* satellite (Obs no. 0101440201, 13/08/2002, PI Pallavicini), so we have searched the 2XMMi-DR3 catalogue to see if any of our candidates are listed here (Watson et al. 2009). We find that the four objects which lie within the *XMM–Newton* field have X-ray counterparts. Their identities and broad-band fluxes (0.5–4.5 keV) are shown in Table 4. To determine if these fluxes are at the levels, we should expect from low-mass stars in IC 2602, we have cross-matched the list of X-ray/optical members from Randich et al. (1995) with the 2XMMi-DR3 catalogue. Four stars from their study, R 57, 58, 64 and 106, lie within the *XMM–Newton* pointing and are recovered with mean broad-band (0.5–4.5 keV) fluxes of $1.4403 \pm 0.1920 \times 10^{-13}$, $1.1475 \pm 0.0080 \times 10^{-12}$, $9.4746 \pm 0.3590 \times 10^{-14}$ and $2.9127 \pm 0.1600 \times 10^{-14}$ mW m^{-2}, respectively.

The ratio between stellar X-ray and bolometric luminosity is observed to increase with decreasing mass, but to eventually reach a saturation point the location of which appears to be dependent on stellar age (e.g. Cargile, James & Platais 2009). For a young population comparable to IC 2602, this occurs at $V - I_C \approx 0.7$–0.9 mag. The four objects from Randich et al. (1995) and our four candidate members have $V - I_C$ in the range 0.77–3.1 mag thus should all lie on this relatively flat part of the L_X/L_{bol} relation,

[5] http://heasarc.nasa.gov/mailarchive/rosnews/msg00129.html

where the spread in X-ray luminosities is a bit less than an order of magnitude ($V - I_C$ for our candidates was estimated on the basis their spectral types and data in table 6 of Leggett 1992).

Using I_C-band bolometric corrections from Monet et al. (1992), we have estimated the logarithm of the bolometric luminosities of 2MASS J10422712−6421401, 2MASS J10420463−6434373, 2MASS J10443357−6415455 and 2MASS J10432126−6419594 to be 27.59, 27.55, 27.36 and 27.13, respectively. Assuming a constant conversion factor between 0.5–4.5 keV flux and X-ray luminosity, we determine that 2MASS J10422712−6421401, 2MASS J10420463−6434373 and 2MASS J10443357−6415455 lie <0.25 dex from the mean of the L_X/L_{bol} values for R 57, 58 and 64. However, both R 106 and 2MASS J10432126−6419594 lie 0.8–0.9 dex below this mean. We conclude that the X-ray fluxes of 2MASS J10422712−6421401 and 2MASS J10420463−6434373 are consistent with them being low-mass cluster members. 2MASS J10443357−6415455 also has an X-ray flux which is indicative of an association with IC 2602 but since our estimated spectral type for this object is ∼1 earlier than that of other candidates of similar magnitude, we have chosen to classify it only as a possible member (see Table 4).

3.4 Proper motions

Proper motions provide a potentially powerful method of discriminating members of a cluster from the general field population (e.g. Hambly, Hawkins & Jameson 1993). There are a number of online data bases which provide these measurements over the bulk of the sky e.g. USNO-B1.0 (Monet et al. 2003), SuperCOSMOS Sky Survey (Hambly et al. 2001), Naval Observatory Merged Astrometric Data set (NOMAD; Zacharias et al. 2004) and PPMXL (Roeser, Demleitner & Schilbach 2010), including the area covered by IC 2602. However, these resources draw heavily on comparatively low spatial resolution photographic plate data, e.g. in the Southern hemisphere from the UKST and the ESO Schmidt telescope. At the relatively low Galactic latitude of IC 2602, crowding becomes an issue and there is a substantial likelihood of a stellar profile being blended with that of another star (or stars). This can lead to systematic error in a proper motion measurement and an inaccurate conclusion about membership status, especially at the fainter magnitudes inhabited by our candidates. For example, IC 2602 has a proper motion as measured by *Hipparcos* of $\mu_\alpha \cos\delta = -17.03 \pm 0.16$, $\mu_\delta = +11.05 \pm 0.15$ mas yr^{-1} (Robichon et al. 1999) so the astrometry reported in NOMAD for 2MASS J10430236−6402132 ($\mu_\alpha \cos\delta = -118.0 \pm 9.0$, $\mu_\delta = +23.9 \pm 9.0$ mas yr^{-1}) and 2MASS J10370251−6444416 ($\mu_\alpha \cos\delta = 499.9 \pm 9.0$, $\mu_\delta = -82.6 \pm 9.0$ mas yr^{-1}) seems to argue strongly that these candidates are very unlikely to be cluster members. However, at the modest resolution of photographic plates, 2MASS J10430236−6402132 is actually a blend of two stars with rather different colours. The photocentre of this blend appears to move to the west with increasing wavelength, 2MASS J10430236−6402132 dominating at the near-IR wavelengths of 2MASS. In the ∼17.7 yr between the UKST *I*-band observation (1982 May 23) and the 2MASS imaging (2000 January 23), 2MASS J10370251−6444416 should have moved almost 9-arcsec east in right ascension but visual inspection of these data sets reveals no discernable shift in the photocentre of this candidate. This object is only marginally blended in the photographic data, so it is not obvious why this particular proper motion measurement is so far in error. There also appear to be some discrepancies in the astrometry from catalogue to catalogue. For example, the proper motion of 2MASS J10454174−6444037 is reported as insignificant in NOMAD but listed in the PPMXL and SuperCOSMOS data bases as $\mu_\alpha \cos\delta = -32.5 \pm 12.2$, $\mu_\delta = +44.8 \pm 12.2$ mas yr^{-1} and $\mu_\alpha \cos\delta = +18.5 \pm 16.9$, $\mu_\delta = -3.6 \pm 17.2$ mas yr^{-1}, respectively. We find that the data from these catalogues are rather unreliable in this part of the sky and thus have chosen not to use these when adjudging the membership status of our candidates.

Nevertheless, in response to the referee's concerns about the membership status of our candidates, we have determined the relative proper motions of a number of key objects (i.e. the ones on either side of the lithium depletion boundary (LDB) and three out of four X-ray detections) using the ESO WFI data and frames acquired with the Focal Plane Imager (FPI) of the AAOmega spectrograph. The FPI is an apogee imaging camera which is mounted in front of the skyward facing field plate of 2dF. It contains a 512 × 512 pixel Kodak KAF-0261E CCD and has a field of view of 2.6 × 2.6 arcmin^2. We acquired 3 × 10 s exposures through a RG630 filter for 2MASS J10422712−6421401, 2MASS J10420463−6434373, 2MASS J10430890−6356228, 2MASS J10430236−6402132 and 2MASS J10432126−6419594 in the twilight prior to the regular AAOmega observing nights of 2010 May 06 and 09. On these evenings, the sky was clear and seeing was favourable, ∼0.9–1.2 arcsec. We reduced the images following standard procedures within the IRAF software environment, namely bias and dark subtraction, flat-fielding, astrometric calibration and co-addition.

For each of these candidates, we used the IRAF routine DAOFIND to determine the positions of reference objects of comparable or greater brightness in the two images. We cross-matched these lists of positions using the STARLINK TOPCAT software. Subsequently, we employed routines in the STARLINK SLALIB library to construct a six coefficient linear transform between the two images of each candidate, where $\geq 3\sigma$ outliers were iteratively clipped from the fits. The proper motion, in pixels, was determined by taking the difference between the observed and predicted location of a candidate in the second epoch imaging. This was then converted into milliarcseconds per year in right ascension and declination using the world coordinate system of the first epoch data set and dividing by the time baseline between the two observations (∼9.23 yr). The relative proper motion vector point diagram for these objects (triangles with error bars) is shown in Fig. 3. The proper motions of known bright cluster members (e.g. Whiteoak 1961) have been obtained from the Third US Naval Observatory CCD Astrograph Catalogue (UCAC3; Zacharias et al. 2010) and are overplotted (open circles). To account for the difference between the relative (our measurements) and the absolute (UCAC3) frames of reference, these have been shifted by +4.5 mas yr^{-1} in right ascension and −3.6 mas yr^{-1} in declination. These offsets were estimated from the absolute proper motions of stars at the faint end of UCAC3 within the survey area, where there is substantial overlap, in terms of magnitude, with our reference stars.

In can been seen that four candidates, 2MASS J10422712−6421401, 2MASS J10420463−6434373, 2MASS J10430890−6356228 and 2MASS J10430236−6402132, are clumped together very close to the known bright cluster stars, supporting our conclusion that these are members of IC 2602. One candidate, 2MASS J10432126−6419594, lies well away from the other four, but this was previously suspected to be a non-member on the basis of spectral type, radial velocity and X-ray flux.

3.5 Lithium

The spectra of the 14 remaining candidate members of IC 2602 have been examined for the presence of the 6707.8-Å lithium absorption

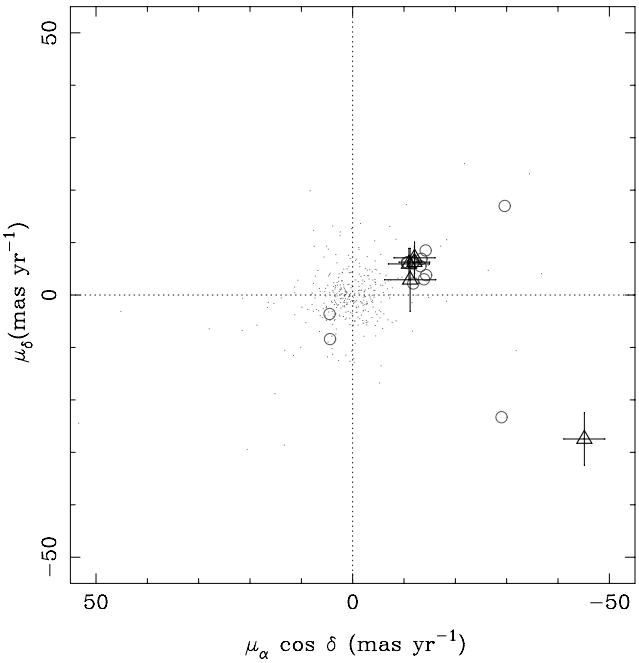

Figure 3. A vector point diagram of the relative proper motions of a number of candidate members of IC 2602 (black triangles with error bars) for which we were able to obtain second epoch CCD imaging. Overplotted are the UCAC3 proper motions of known bright cluster members (grey open circles), shifted to account for the difference between the relative and absolute frames of reference. The relative proper motions of other objects within the FPI fields are also shown (small dots).

line. Compelling evidence of this feature is found in the spectra of six objects (see Table 3). We have used the SPLOT routine in IRAF to measure the EW of the line in these six spectra and also to set upper limits on the EW in the remaining data sets where there is no convincing detection. The results of these measurements are shown in Table 3.

Of note, we find two objects with clear detections of the 6707.8-Å line that are substantially brighter than the four other lithium rich candidates. The location of these objects approximately +0.75 mag above the sequence defined by the bulk of the spectroscopic members seen in Fig. 1 could indicate that these two objects are near equal mass binary stars. We might expect to detect one or two binary members in a sample of this size since the binary fraction of low-mass field and open cluster stars is estimated to be ∼30 per cent (Leinert et al. 1997; Pinfield et al. 2003). Of course, with the available data we cannot exclude the possibility that these are simply young field star interlopers (indeed the referee has suggested that they may be related to the Lower Centaurus Crux association) but their spectral classifications are consistent with the binary hypothesis.

Lithium is positively detected in the spectra of all four candidate members fainter than 2MASS J10430890−6356228, which has $J = 14.04 \pm 0.03$ mag ($K_S = 13.17 \pm 0.04$ mag). The brightest lithium-rich candidate with a position in the CMD which is consistent with the single star sequence defined by the other members is 2MASS J10439236−6402132, which has $J = 14.25 \pm 0.05$ mag ($K_S = 13.30 \pm 0.04$ mag). Following Manzi et al. (2008), on the basis of the photometry of these two objects we conclude that the lithium depletion boundary of IC 2602 lies within the range $J = 14.01$–14.30 mag ($K_S = 13.13$–13.34 mag), allowing for the uncertainties in the 2MASS photometry. Spectroscopy around the 6707.8-Å line

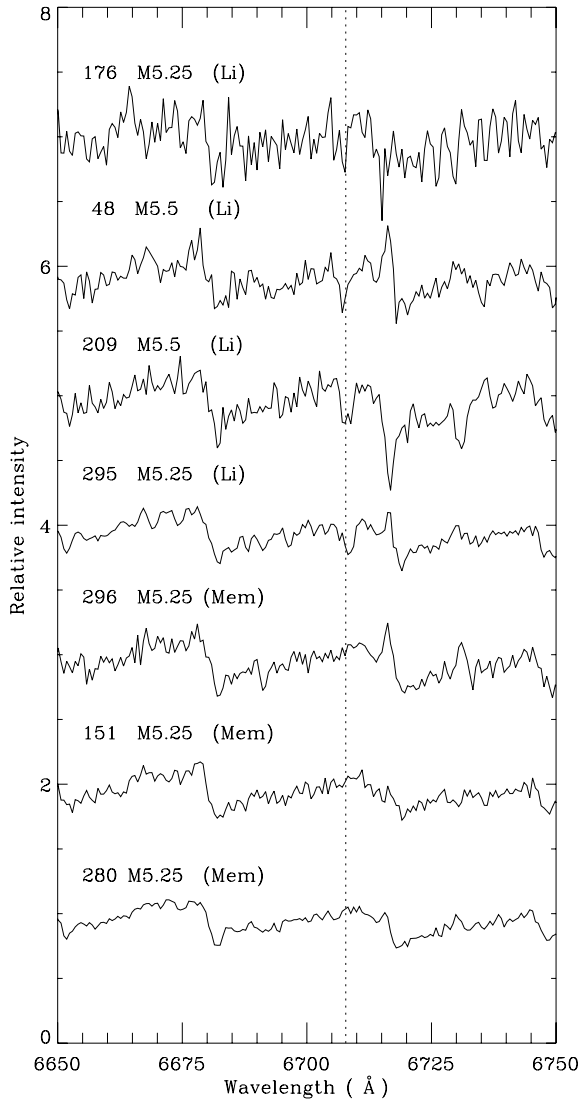

Figure 4. AAOmega optical spectroscopy centred around 6700 Å for seven probable members located closest to the lithium depletion boundary (labelled by fiber number – see Table 2). The lithium absorption line at 6707.8 Å can be clearly seen in the top four data sets, corresponding to the four faintest stars.

for the four objects closest to either side of the lithium depletion boundary is shown in Fig. 4. In the next section, we will use this result to place new constraints on the age of the cluster.

4 DISCUSSION

Our photometric and spectroscopic survey of IC 2602 has led to the discovery of two possible and 12 probable new members. These are the lowest mass objects in this cluster reported to date with $M \lesssim 0.3\,\mathrm{M}_\odot$ (assuming an age of $\tau \sim 50$ Myr as derived below). We can place a constraint on the luminosity function (LF) of IC 2602 over the range $M_J = 7.30$–9.60 mag of LF (number of objects) $>(12-\sqrt{12})/2.3 \approx 3.7\,\mathrm{mag}^{-1}$. This is strictly a lower limit since, first, we have not surveyed the whole area spanned by the cluster on the sky. Secondly, our photometric selection was somewhat of a compromise to keep the number of objects for spectroscopic follow-up to a manageable number and ideally for completeness would have pushed further into the field stars. Thirdly, we may have rejected the

faintest members observed spectroscopically as the poorer signal-to-noise ratio of these data sets may not have clearly revealed Hα emission. Finally, not all photometric candidates were allocated a fibre for spectroscopic follow-up.

Nevertheless, the new low-mass cluster members we have identified have allowed us to pin down the location of the lithium depletion boundary to $J = 14.01$–14.30 mag ($K_S = 13.13$–13.34 mag) and allowed us to place improved constraints on the age of IC 2602. As demonstrated by Jeffries & Oliveira (2005) in their investigation into the age of NGC 2457, there is an excellent level of agreement amongst theoretical models about the rate at which lithium is consumed in low-mass stars and brown dwarfs. Thus ages derived from the lithium depletion boundary appear to be relatively insensitive to the choice of stellar evolutionary model. Additionally, both Jeffries & Oliveira (2005) and Manzi et al. (2008) clearly show that over the range $\tau \sim 25$–50 Myr, lithium depletion boundary ages derived using the theoretical near-IR magnitudes of Baraffe et al. (1998) are in very good agreement with estimates obtained using bolometric corrections and magnitudes. Since the calibration of our I-band photometry may be open to question, we have estimated the lithium depletion boundary age for IC 2602 using only the derived M_J and M_K magnitudes of the boundary and the theoretical near-IR photometry of Baraffe et al. (1998).

To derive these absolute magnitudes, we have adopted a distance modulus of $(m - M)_0 = 5.86 \pm 0.1$. This is based on the most recent *Hipparcos* determination and is consistent with the majority of distance estimates in the literature (Braes 1961; Whiteoak 1961; Robichon et al. 1999; van Leeuwen 2009). We have assumed reddening of $A_J = 0.03$ and $A_K = 0.01$ based on $E(B - V) = 0.035$ (Hill & Perry 1969) and $A_J/E(B - V) = 0.86$ and $A_K/E(B - V) = 0.36$ (Fitzpatrick 1999). We have also considered the finite depth of the cluster since it is effectively a further uncertainty on the distance to each individual member. Whiteoak (1961) notes that the bright stellar members are located within a region $\sim 1\overset{\circ}{.}5$ in diameter. While IC 2602 is perhaps not yet old enough to have fully reached a state of energy equipartition, the low-mass stellar members will likely be more widely distributed due to dynamical effects. In the dynamically relaxed Pleiades, the low-mass stars have approximately twice the core radius of the intermediate mass stars (Pinfield, Jameson & Hodgkin 1998). Crudely extrapolating this result to IC 2602, we estimate that most low-mass stars should lie within 4 pc of the cluster centre which corresponds to ± 0.06 on the distance modulus of individual members. Adding the uncertainties in quadrature we estimate that the LDB in IC 2602 occurs within the range $M_J = 8.03$–8.49 mag and $M_K = 7.17$–7.56 mag.

These ranges have been compared to the theoretical predictions of the Lyon group (Chabrier & Baraffe 1997; Baraffe et al. 1998) for M_J and M_K as a function of age, at which 99 per cent of a stars primordial lithium has been burned. These synthetic magnitudes have been moved on to the 2MASS system using the transforms of Carpenter (2001) and cubic splines have been used to interpolate between points in the model tables. Based on the J and the K_S photometric bands, we have determined $\tau = 46.2^{+6}_{-5}$ and $\tau = 46.6^{+5}_{-4}$ Myr, respectively (Fig. 5) and thus we conclude that the age of IC 2602 is $\tau = 46^{+6}_{-5}$ Myr. This LDB derived age is larger by a factor of $\sim$1.8 than the age ($\tau = 25$ Myr; Stauffer et al. 1997) obtained by comparing the position in the Hertzsprung–Russell (HR) diagram of the low-mass cluster sequence to the predictions of the models of D'Antona & Mazzitelli (1994). It is greater by a factor of $\sim$1.3 than the MSTO age of $\tau = 35$ Myr determined by Mermilliod (1981) using stellar evolutionary models which allowed for modest levels of convective core overshoot (Maeder & Mermilliod 1981). It is also larger by a factor of $\sim$1.4 than the age of the NextGen model which, despite some suggestion from Fig. 1 of some systematic error which is likely related to the I-band colour transform, provides a reasonable match to the location of probable cluster members on either side of the LDB in the J, $I - J$ CMD (see Fig. 1), reinforcing the claim by Jeffries & Oliveira (2005) that stars with $I - J > 1.5$ appear to drift towards younger ages in CMDs. Conversely, Kharchenko et al. (2005) have determined an MSTO age of $\tau = 67$ Myr using the more recent evolutionary models of Girardi et al. (2000). However, this is based on the location in the HR diagram of just two stars and should also be taken in the context of their age estimate for IC 2391 of $\tau = 75$ Myr (also based on just two stars). Thus we believe that IC 2602 is consistent with the general trend delineated by the Pleiades, α-Per, IC 2391 and NGC 2457, whereby

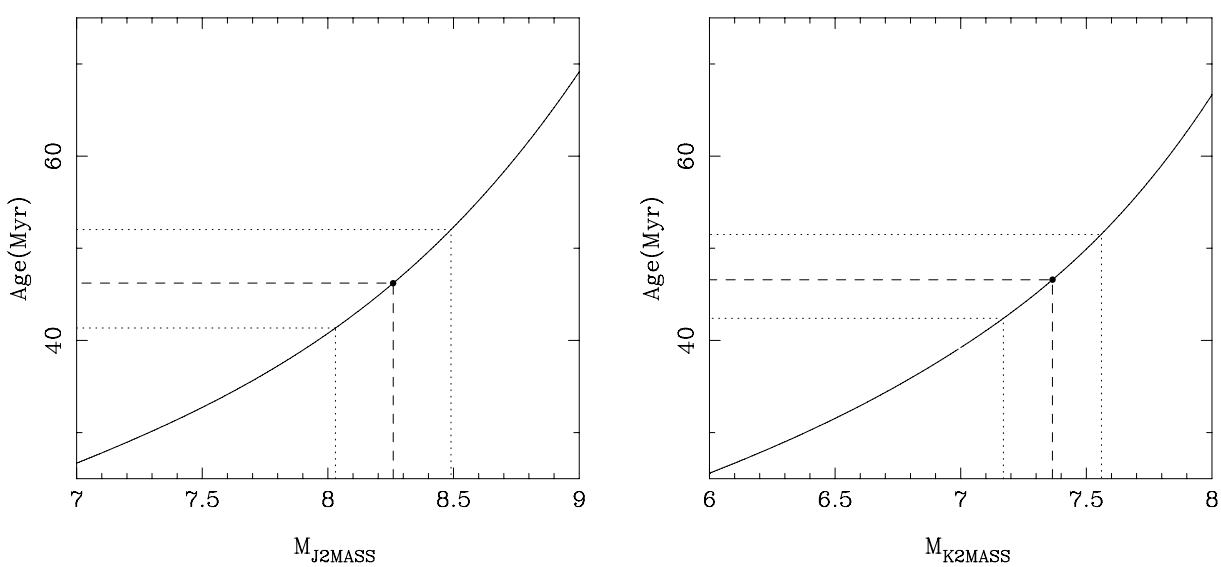

Figure 5. Theoretically predicted relationships between age and absolute J and K_S magnitudes for a 99 per cent level of lithium depletion (Chabrier & Baraffe 1997; Baraffe et al. 1998). Our determination of the LDB in terms of magnitude and age is highlighted (dashed lines) as are our estimated uncertainties on this (dotted lines).

the LDB age is ∼120–160 per cent of the estimates derived using more traditional techniques. This trend is only currently bucked by IC 4665 where the MSTO age determination ($\tau = 36$ Myr; Mermilliod 1981) is larger than the LDB age by a factor of ∼1.3 (see Manzi et al. 2008).

Adopting our new age estimate, we can now place limits on the cluster mass function around the LDB. At $\tau = 46$ Myr, according to the NextGen models of Baraffe et al. (1998), $M_J = 7.30$–9.60, the range covered by our spectroscopic follow-up, corresponds to a mass interval of $M = 0.054$–$0.24\,\mathrm{M}_\odot$. Based on our new limits on the luminosity function, we determine $\mathrm{d}n/\mathrm{d}M > 46\,\mathrm{M}_\odot^{-1}$ over this mass range. This is marginally less than the value we derive for the mass function in the range $M = 0.43$–$0.72\,\mathrm{M}_\odot$ based on the lowest mass candidate members published by Randich et al. (2001). This supports the supposition that our estimate is strictly a lower limit. Nevertheless, if the mass function of IC 2602 has a similar form to that of other young open clusters and associations ($\mathrm{d}n/\mathrm{d}M \propto M^{-\alpha}$, $\alpha = 0.6$–0.8, e.g. Béjar et al. 2001; Lodieu et al. 2007b), based on this number we can expect at the very least a handful of brown dwarf members in future wide, deep near-IR surveys. With low foreground reddening and a greatly improved age determination now available for IC 2602, these can potentially serve as benchmark objects (e.g. Pinfield et al. 2006).

Finally, we suggest that it may be possible to determine an LDB age for a number of other clusters using relatively modest sized telescopes. If clean samples of members of well populated clusters with modest foreground reddening can be isolated either via proper motion or radial velocity, then the spectra of several to tens of members, depending on the richness, could be stacked to boost the signal-to-noise ratio of the data to the levels necessary to study the 6707.8-Å lithium line. An approach of this sort might place an LDB age for the cluster Blanco 1 within the reach of the AAT and AAOmega.

5 CONCLUSIONS

We have performed a photometric and spectroscopic survey of $\sim 1.4\,\mathrm{deg}^2$ of the young cluster IC 2602. This has unearthed two possible and 12 probable new cluster members with masses in the range $M = 0.1$–$0.24\,\mathrm{M}_\odot$. These are the lowest mass members of the cluster found to date. We have used the lithium depletion boundary technique to place improved constraints on the age of IC 2602, $\tau = 46^{+6}_{-5}$ Myr, and determined a lower limit to the cluster mass function, $\mathrm{d}n/\mathrm{d}M > 46\,\mathrm{M}_\odot^{-1}$, over $M = 0.054$–$0.24\,\mathrm{M}_\odot$. If the mass function of IC 2602 has a form comparable to that of other young clusters and associations, we estimate the cluster will contain at least a handful of brown dwarfs. These objects will be within the reach of the new generation of near-IR survey instruments e.g. Visible and Infrared Survey Telescope for Astronomy (VISTA), and, given the availability of an LDB age for this population, may prove useful as further benchmark brown dwarfs.

For completeness, we will provide the coordinates and photometry of all objects observed with AAOmega, as well as a hard copy of the reduced optical spectra via a webpage.[6]

ACKNOWLEDGMENTS

NL acknowledges funding from the Spanish Ministry of Science and Innovation through the Ramón y Cajal fellowship number 08-303-01-02. NL extends his gratitude to the Anglo-Australian Observatory (AAO) for part funding his visit to Epping and to the AAO staff for an enjoyable stay. We thank Kevin Luhman for providing the optical spectra of young objects in η Chamaeleontis and Isabelle Baraffe for supplying the evolutionary models in a form suitable for this work. We also thank Simon O'Toole for helpful tips on the use of fxcorr, Steve Lee for help in acquiring the FPI imaging, Kevin Pimmblet (GAMA) for allowing us to observe during evening twilight and the anonymous referee for comments which have improved this paper.

Based on data obtained with the AAOmega fibre-fed optical spectrograph at the AAO under program AATAC/10A/27. Based on observations made with ESO Telescopes at the La Silla Paranal Observatory under programme number 66.D-0335(A) and retrieved from the ESO Science Archive Facility.

This research has made use of the Simbad data base, operated at the Centre de Données Astronomiques de Strasbourg (CDS), and of NASA's Astrophysics Data System Bibliographic Services (ADS). This publication has also made use of data products from the Two Micron All Sky Survey, which is a joint project of the University of Massachusetts and the Infrared Processing and Analysis Center/California Institute of Technology, funded by the National Aeronautics and Space Administration and the National Science Foundation.

[6] www.iac.es/galeria/nlodieu/publications/

REFERENCES

Baade D. et al., 1999, Messenger, 95, 15
Baraffe I., Chabrier G., Allard F., Hauschildt P. H., 1998, A&A, 337, 403
Barnes J. R., Collier Cameron A., James D. J., Steeghs D., 2001, MNRAS, 326, 1057
Barnes S. A., Sofia S., Prosser C. F., Stauffer J. R., 1999, ApJ, 516, 263
Barrado y Navascués D., Stauffer J. R., Patten B. M., 1999, ApJ, 522, L53
Barrado y Navascués D., Bouvier J., Stauffer J. R., Lodieu N., McCaughrean M. J., 2002, A&A, 395, 813
Barrado y Navascués D., Stauffer J. R., Jayawardhana R., 2004, ApJ, 614, 386
Basri G., Marcy G. W., Graham J. R., 1996, ApJ, 458, 600
Béjar V. J. S. et al., 2001, ApJ, 556, 830
Braes L. L. E., 1961, Monthly Notes Astron. Soc. South Africa, 20, 7
Cargile P. A., James D. J., Platais I., 2009, AJ, 137, 3230
Carpenter J. M., 2001, AJ, 121, 2851
Chabrier G., 2003, PASP, 115, 763
Chabrier G., Baraffe I., 1997, A&A, 327, 1039
Claret A., 1997, A&AS, 125, 439
Cruz K. L., Reid I. N., 2002, AJ, 123, 2828
Cutri R. M. et al., 2003, 2MASS All Sky Catalog of point sources, 2246
D'Antona F., Mazzitelli I., 1994, ApJS, 90, 467
Dobbie P. D., Kenyon F., Jameson R. F., Hodgkin S. T., Pinfield D. J., Osborne S. L., 2002, MNRAS, 335, 687
Dobbie P. D. et al., 2006, MNRAS, 369, 383
Dobbie P. D., Napiwotzki R., Burleigh M. R., Williams K. A., Sharp R., Barstow M. A., Casewell S. L., Hubeny I., 2009, MNRAS, 395, 2248
Fitzpatrick E. L., 1999, PASP, 111, 63
Foster D. C., Byrne P. B., Hawley S. L., Rolleston W. R. J., 1997, A&AS, 126, 81
Girardi L., Bressan A., Bertelli G., Chiosi C., 2000, A&AS, 141, 371
Hambly N. C., Hawkins M. R. S., Jameson R. F., 1993, A&AS, 100, 607
Hambly N. C. et al., 2001, MNRAS, 326, 1279
Hill G., Perry C. L., 1969, AJ, 74, 1011
Irwin M., Lewis J., 2001, New Astron. Rev., 45, 105
Irwin J., Hodgkin S., Aigrain S., Bouvier J., Hebb L., Irwin M., Moraux E., 2008, MNRAS, 384, 675
Irwin J., Aigrain S., Bouvier J., Hebb L., Hodgkin S., Irwin M., Moraux E., 2009, MNRAS, 392, 1456

Jeffries R. D., James D. J., 1999, ApJ, 511, 218
Jeffries R. D., Oliveira J. M., 2005, MNRAS, 358, 13
Jeffries R. D., Oliveira J. M., Barrado y Navascués D., Stauffer J. R., 2003, MNRAS, 343, 1271
Kalirai J. S., Richer H. B., Reitzel D., Hansen B. M. S., Rich R. M., Fahlman G. G., Gibson B. K., von Hippel T., 2005, ApJ, 618, L123
Kharchenko N. V., Piskunov A. E., Röser S., Schilbach E., Scholz R.-D., 2005, A&A, 438, 1163
Kharchenko N. V., Scholz R., Piskunov A. E., Röser S., Schilbach E., 2007, Astron. Nachr., 328, 889
King J. R., Schuler S. C., Hobbs L. M., Pinsonneault M. H., 2010, ApJ, 710, 1610
Kroupa P., 2002, Sci, 295, 82
Leggett S. K., 1992, ApJS, 82, 351
Leinert C., Henry T., Glindemann A., McCarthy D. W., Jr, 1997, A&A, 325, 159
Lewis I. J. et al., 2002, MNRAS, 333, 279
Lodieu N., Dobbie P. D., Deacon N. R., Hodgkin S. T., Hambly N. C., Jameson R. F., 2007a, MNRAS, 380, 712
Lodieu N., Hambly N. C., Jameson R. F., Hodgkin S. T., Carraro G., Kendall T. R., 2007b, MNRAS, 374, 372
Lodieu N., Zapatero Osorio M. R., Rebolo R., Martín E. L., Hambly N. C., 2009, A&A, 505, 1115
Luhman K. L., 2004, ApJ, 616, 1033
Luhman K. L., Steeghs D., 2004, ApJ, 609, 917
Maeder A., Mermilliod J. C., 1981, A&A, 93, 136
Manzi S., Randich S., de Wit W. J., Palla F., 2008, A&A, 479, 141
Marsden S. C., Waite I. A., Carter B. D., Donati J., 2005, MNRAS, 359, 711
Marsden S. C., Carter B. D., Donati J., 2009, MNRAS, 399, 888
Mermilliod J. C., 1981, A&A, 97, 235
Meynet G., Mermilliod J., Maeder A., 1993, A&AS, 98, 477
Miszalski B., Shortridge K., Saunders W., Parker Q. A., Croom S. M., 2006, MNRAS, 371, 1537
Monet D. G., Dahn C. C., Vrba F. J., Harris H. C., Pier J. R., Luginbuhl C. B., Ables H. D., 1992, AJ, 103, 638
Monet D. G. et al., 2003, AJ, 125, 984
Moraux E., Bouvier J., Clarke C., 2005, Astron. Nachr., 326, 985
Naylor T., Totten E. J., Jeffries R. D., Pozzo M., Devey C. R., Thompson S. A., 2002, MNRAS, 335, 291
Nicolet B., 1981, A&A, 104, 185
Oliveira J. M., Jeffries R. D., Devey C. R., Barrado y Navascués D., Naylor T., Stauffer J. R., Totten E. J., 2003, MNRAS, 342, 651
Pan X., Shao M., Kulkarni S. R., 2004, Nat, 427, 326
Parker Q. A. et al., 2005, MNRAS, 362, 689
Pillitteri I., Micela G., Reale F., Sciortino S., 2005, A&A, 430, 155
Pinfield D. J., Jameson R. F., Hodgkin S. T., 1998, MNRAS, 299, 955
Pinfield D. J., Dobbie P. D., Jameson R. F., Steele I. A., Jones H. R. A., Katsiyannis A. C., 2003, MNRAS, 342, 1241
Pinfield D. J., Jones H. R. A., Lucas P. W., Kendall T. R., Folkes S. L., Day-Jones A. C., Chappelle R. J., Steele I. A., 2006, MNRAS, 368, 1281
Pinsonneault M., 1997, ARA&A, 35, 557
Prosser C. F., Randich S., Stauffer J. R., 1996, AJ, 112, 649
Randich S., Schmitt J. H. M. M., Prosser C. F., Stauffer J. R., 1995, A&A, 300, 134
Randich S., Aharpour N., Pallavicini R., Prosser C. F., Stauffer J. R., 1997, A&A, 323, 86
Randich S., Pallavicini R., Meola G., Stauffer J. R., Balachandran S. C., 2001, A&A, 372, 862
Rebolo R., Martín E. L., Magazzù A., 1992, ApJ, 389, L83
Reid I. N., Hawley S. L., Gizis J. E., 1995, AJ, 110, 1838
Robichon N., Arenou F., Mermilliod J.-C., Turon C., 1999, A&A, 345, 471
Roeser S., Demleitner M., Schilbach E., 2010, AJ, 139, 2440
Saunders W. et al., 2004, Proc. SPIE, 5492, 389
Sharp R. et al., 2006, Proc. SPIE, Vol. 6269, 62690G
Skrutskie M. F. et al., 2006, AJ, 131, 1163
Stauffer J. R., Hamilton D., Probst R. G., 1994, AJ, 108, 155
Stauffer J. R., Hartmann L. W., Prosser C. F., Randich S., Balachandran S., Patten B. M., Simon T., Giampapa M., 1997, ApJ, 479, 776
Stauffer J. R., Schultz G., Kirkpatrick J. D., 1998a, ApJ, 499, L219
Stauffer J. R., Schild R., Barrado y Navascues D., Backman D. E., Angelova A. M., Kirkpatrick J. D., Hambly N., Vanzi L., 1998b, ApJ, 504, 805
van Leeuwen F., 2009, A&A, 497, 209
Watson M. G. et al., 2009, A&A, 493, 339
Weidemann V., 2000, A&A, 363, 647
West A. A., Hawley S. L., Bochanski J. J., Covey K. R., Reid I. N., Dhital S., Hilton E. J., Masuda M., 2008, AJ, 135, 785
Whiteoak J. B., 1961, MNRAS, 123, 245
Williams K. A., Bolte M., Koester D., 2004, ApJ, 615, L49
Woo J., Demarque P., 2001, AJ, 122, 1602
Zacharias N., Urban S. E., Zacharias M. I., Wycoff G. L., Hall D. M., Monet D. G., Rafferty T. J., 2004, AJ, 127, 3043
Zacharias N. et al., 2010, AJ, 139, 2184

This paper has been typeset from a TEX/LATEX file prepared by the author.